BEAMFORMING FOR THERAPY WITH HIGH INTENSITY FOCUSED ULTRASOUND (HIFU) USING QUANTITATIVE SCHLIEREN

C. I. ZANELLI*, S. DeMARTA**, C. W. HENNIGE** and M. M. KADRI*

*Intec Research Company, Sunnyvale, CA 94089
**Focal Surgery, Milpitas, CA 95035

Abstract

The requirements for beamforming in high intensity focused ultrasound (HIFU) for tissue destruction are substantially different than those for diagnostic imaging. High numerical aperture and CW efficiency are desirable for tissue destruction, while depth of focus and broadband sensitivity are key to good imaging. When the same transducer must be used for ablation *and* imaging some compromises must be made, resulting in non-ideal beam patterns. Predicting the dosage in tissue that results from actual beam patterns becomes a key element in designing such systems. Quantitative schlieren images in CW mode are used to provide fast, high dynamic range field maps in water. The image data are then corrected for attenuation, resulting in simulated beam profiles and absorbed dose rates for tissue.

Introduction

High intensity focused ultrasound (HIFU) is a well-known technique to deposit large amounts of energy in a localized region without affecting intervening tissue[1-3]. In recent years, after the development of low-loss ceramics, its therapeutic value has been revisited because of its potential to perform subcutaneous surgery. This approach (sometimes refered to as ablation) requires intensities of the order of 1 KW/cm^2 that raise the temperature of tissue to 70-80°C and higher (as opposed to 40-45°C, as required for hyperthermia), effectively destroying the cells by denaturing their protein content. Subsequently, the dead cells are removed by surrounding perfusion.

To generate such high intensities, a highly focused CW beam is produced by a large aperture transducer, as shown in figure 1. A generally used figure of merit is the net acoustic intensity gain, resulting from focusing and attenuation, defined as the ratio of intensities at the surface of the transducer and at the focal point.

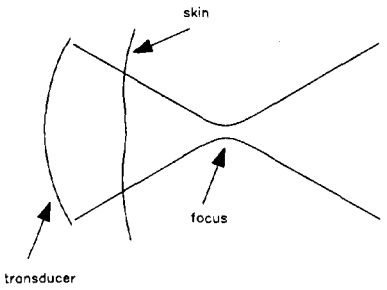

Figure 1. Geometry in HIFU applications.

The intensity as a function of distance from the transducer can be calculated based on beam geometry, under the assumption of spherical waves of uniform amplitude, as shown in figure 2. The net gain is easily obtained from this curve, and frequency can be selected for the highest gain (see Appendix).

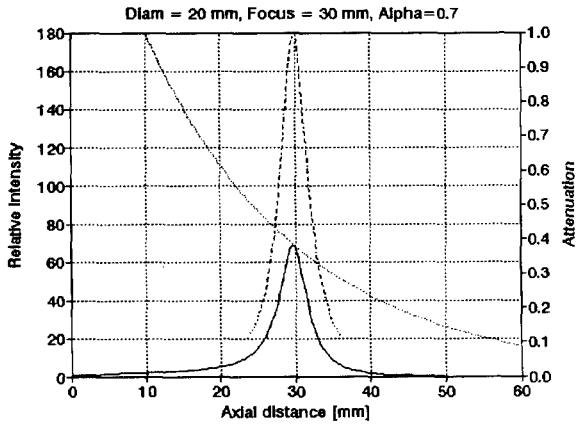

Figure 2. Example of net intensity gain (solid line) as the product of geometric gain (dashes) and attenuation (dots).

However, actual beams are rarely uniform. In particular, when part of the transducer is used for imaging, the radiative surface is no longer homogeneous, and the wave

1051-0117/93/0000-1233 $4.00 © 1993 IEEE

is not spherical. Diffraction theory applies only partially, and one must recur to actual beam measurements.

Field measurements

Measuring the acoustic field is a slow process, requiring very fine sampling especially near the focal spot. In our case[4] the beam waist is about 0.5 mm in diameter, while the smallest available hydrophones have an effective diameter of 0.3 mm. Measurements made with a hydrophone that is so large provide an inaccurate description of the focal spot and the field intensities, effectively averaging over its sensing area. In our case, the large transducer aperture requires further corrections for hydrophone directivity. Hydrophones are also limited to measurements at low intensities due to their fragility, and sturdy designs are large, causing stationary waves when used in CW mode.

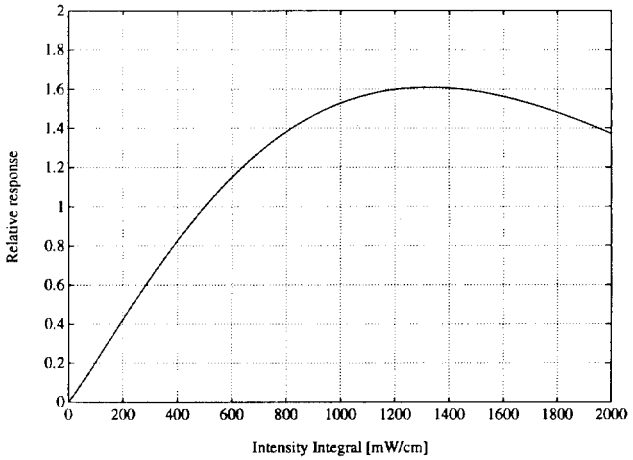

Figure 3. Schlieren calibration curve. See text.

In the present work we have made use of quantitative schlieren, which allows sampling the beam with a resolution of 0.1 mm, with the advantage of being non-intrusive to the acoustic field. A description of the schlieren apparatus can be found in reference [5], and its response calibration curve is shown in figure 3. The calibration curve indicates that measurements at line-integral intensities of up to 1000 mW/cm are reasonable. Note that the units are mW/cm and not mW/cm^2. This is because the acousto-optic system integrates sound pressure along the light path, so intensity values are not readily available except after deconvolution. A simple form of deconvolution to obtain an intensity map can be done under some limited symmetry conditions[6], and it works well for cylindrical beams of monotonic (bell-shaped) profiles. More complex deconvolution is required for the general case[7].

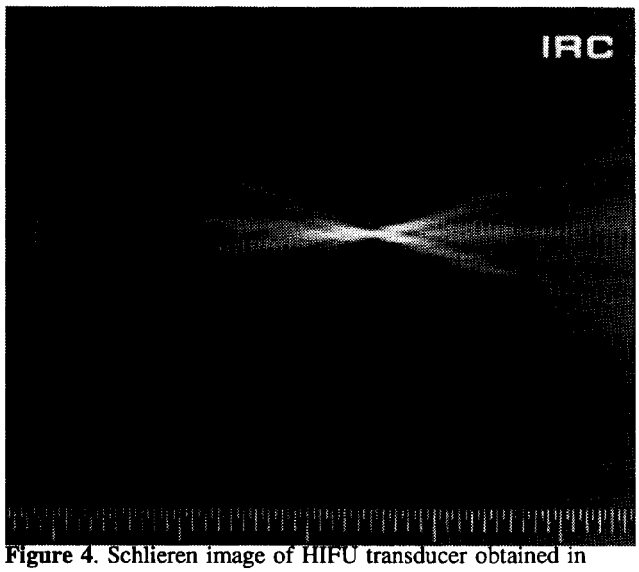

Figure 4. Schlieren image of HIFU transducer obtained in water.

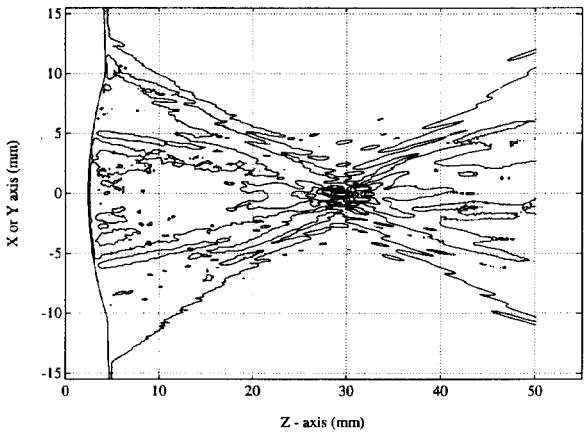

Figure 5. Contour representation of the schlieren image.

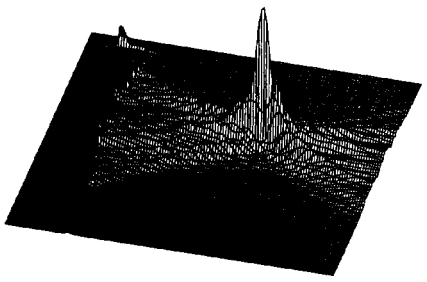

Figure 6. 3D representation of the intensity integral measured in water.

A typical image of the field is shown in figure 4. The brightness at each location has been linearized to correspond to a line-integral intensity value. Figure 5 depicts the same data in contour form, and figure 6 is a 3-D mesh where intensity values are indicated by height. Although high dynamic range digitization of the image is possible, two images were composed into one to obtain a dynamic range of about 40 dB.

Geometry

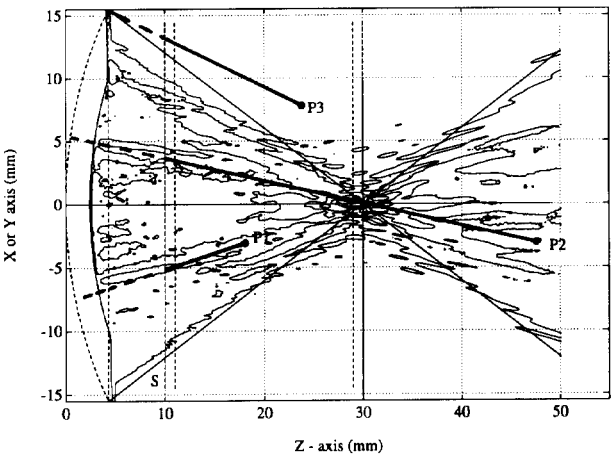

Figure 7. Geometry of the beam overlayed to schlieren contour map.

The location of the transducer and acoustic field relative to it are obtained directly from the schlieren image. The main geometric elements, based on the contour map, are shown in figure 7. The skin (S) is modeled as a flat interface, located at a fixed distance from the transducer and perpendicular to the beam axis, beyond which the sound is attenuating uniformly. The distance from the center of the transducer bowl to the skin plane (water standoff) as well as its curvature, can be adjusted in the model.

Attenuation

The schlieren image is obtained in water, thus it does not represent the situation in tissue. To estimate the beam in tissue, we have used a method similar to that described in reference [8] to define regions in which the mean acoustic path through tissue is calculated. Although a more detailed calculation by surface integration is possible, the complexity of such calculation is not warranted since the inhomogeneities of tissue will probably result in larger variations.

The dose rate (amount of power deposited per unit mass) as any point r is

$$D(r) = (1/\rho)\ \eta\ I(r) \qquad (1)$$

where η is the absorption coefficient (in nepers/unit length), ρ is the density of tissue, and $I(r)$ the acoustic intensity at that location.

The most challenging part of accurately simulating the phenomena underlying tissue ablation deals with the inclusion of non-linear attenuation and thermal effects. This is because the sound velocity and absorption coefficient are temperature-dependent, and temperature, in turn, is controlled by the dose absorbed by the affected tissue.

It is generally assumed that η is a constant, although it is well known that for HIFU applications this is not the case. In general, for high intensities the non-linear behavior of tissue and the changes in its physical constitution as temperature increases lead to expressing the absorption coefficient as

$$\eta(r) = \eta\{I(r),T(r)\} \qquad (2)$$

where $T(r)$ is the temperature at point r. To understand this dependence requires a knowledge of the tissue structure that is beyond the scope of this work, but phenomenological descriptions of this dependency can be readily included in the simulation.

Clearly since $T(r)$ is dependent on the absorbed dose and the thermal conductivity of the tissue --including perfusion-- knowing the functional form of eq. (2) would allow simulations along the dimension of time.

Simulation

The actual wave amplitude at any point ***P*** is the result of the integral sum of all contributions along the paths connecting ***P*** with the source, so a detailed calculation would involve knowing all the contributions (phase and magnitude) that make up the beam at any given location, and applying attenuation along each path. We do not have such detailed set of data for a real device to make this computation. Assumptions can be made for an ideal transducer, but it defeats the purpose of using real data. Even if we had a map of phase and magnitude at the

transducer face, however, the processing would be too lengthy except perhaps for a fast vector processing computer. For a mildly focused beam the attenuation is computed based on the tissue path traversed by the sound along the direction of the beam axis, with very good results. Simulating the attenuation of a highly focused wave requires some approximations.

The first approximation consists of assuming that most of the beam is contained within a cone emerging from the transducer surface, converging towards the center of curvature, and then diverging away from the transducer (see figure 7). Within this double cone, the attenuation path to a given point P is computed as follows: the line that connects the point and the center of curvature (geometric focus) is extrapolated to intercept the water/tissue (skin) interface (P_1, P_2). The attenuative path is then the distance between this skin intercept and the point at which the value is computed. For a point outside this cone (P_3), the attenuative path is computed by connecting P_3 to the closest point in the transducer, and the attenuative distance is measured between P_3 and the intercept of this ray and the skin.

This method is slightly inaccurate beyond the focus because the acoustical path has a discontinuity: the tissue path for a point at the inside edge of the cone is longer than that at the outside edge of the cone. Several variations on this method yield similar results, and given the enormous variability in tissue characteristics, the differences are not worth further exploration at this point. In the case of a 2.5 cm focus transducer, this effect is about 4%, which is acceptable for the simulation at hand. We have tried other methods to overcome this difficulty, but implementation is computationally impractical with the present hardware.

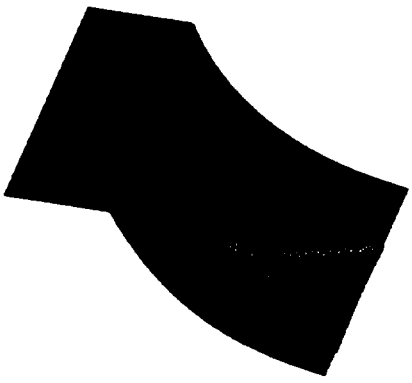

Figure 8. 3D representation of the attenuation function.

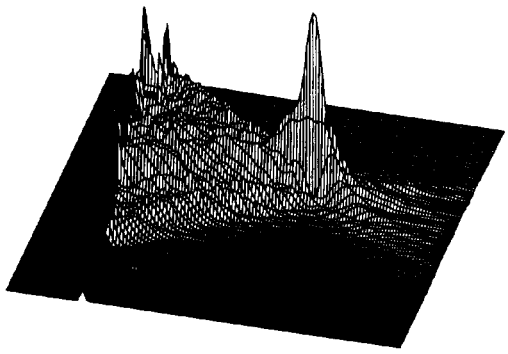

Figure 9. Attenuated beam in 3D representation.

Figure 8 shows the attenuating function as a 3-D mesh. This function is multiplied by the image (figure 4) and the result is shown in figure 9.

Figures of merit

Having determined the in-situ acoustic field, we need to extract information in a more compact form that can be used to modify the beam pattern for optimal therapeutic results. Several parameters have been identified as critical in therapy, and based on this knowledge we isolate them as figures of merit to compare beam patterns:

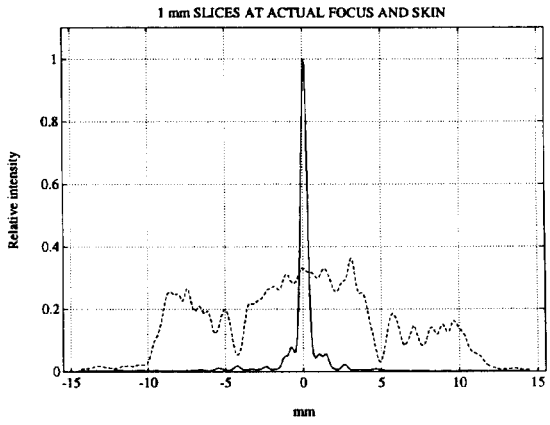

Figure 10. Transversal beam profiles at the peak and at the skin, after attenuation.

Peak-to-skin dose ratio. One of the most important parameters is the ratio between dose at the actual focus and dose anywhere else in tissue --particularly at the skin interface. The dose can vary significantly given the complex structure of the beam, although the tissue probably tends to average its effects due to mild defocusing (phase randomization) and thermal conduction. For this reason, 1-mm slices in the plane perpendicular to the beam propagation are taken where tissue starts and at the actual focus. Intensity profiles are computed by averaging across these swaths (see figure 10).

TAP at focus. This is the dose rate (amount of power delivered) at the focal plane for a given amount of acoustical power delivered by the transducer into the water. The power at the focal zone is calculated as a fraction of the total output power from the transducer. This parameter, *TAP at focus as a percentage of free-field TAP*, is an indication of the efficiency of the HIFU method to deliver power to the focal plane. This number is shown at the top of the transversal profile (figure 10).

Axial Profiles. The acoustic intensity along the axial direction is also of interest to understand the dose distribution in tissue. Four measures of the intensity distribution (see figure 11) are used to assess the dose along the beam path:

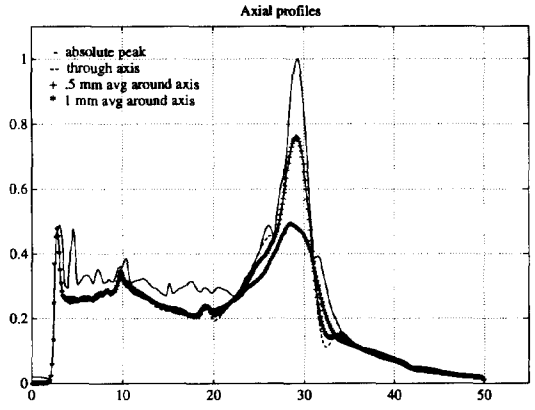

Figure 11. Axial profiles after attenuation.

1. The maximum intensity anywhere in the plane that intersects the beam axis at a fixed distance from the transducer.
2. The intensity over a line as wide as the resolution of the image (~100μm).
3. Average intensity over a 0.5 mm wide swath at the beam axis.
4. Average intensity over a 1.0 mm wide swath at the beam axis.

Limitations

The main difference between the intensity measured in water and that found in therapy is caused by absorption, and this is what the present simulation addresses. However, there are other differences which, depending on the application, are not all negligible. Among the effects **not** considered in the present model:

- **multiple reflections** between tissue and transducer
- **refraction** at the water/tissue interface
- **beam scattering** due to tissue inhomogeneities

Effects that can be included, although not yet attempted, are

- **non-linear behavior of tissue**: η depends on acoustic intensity
- **changes in** η due to heating

Conclusions

Within the restrictions described, the model provides a first approximation to the actual in-situ fields, based on actual beam data.

There are some elements of the simulation, however, that may be improved upon. The attenuation coefficient, for instance, represents an average for numerous in-vitro measruements, and does not account for the variability of this figure within the tissue and from patient to patient. A method of assessing this parameter, even as an average for a given patient, will help significantly towards gaining confidence in the results of the simulation.

A second aspect that plays a significant role in this simulation is the location of the skin interface relative to the transducer. Most ultrasonic images suggest that the orientation is not always optimally normal to the incidence of the wave. It would be a significant improvement over the present state of affairs if the shape of the skin surface, as measured by a B-scan image, could be fed directly into the simulation. The calculated dose could then be fed back to the scanned image as a color overlay, and have the simulation recommend a power level based on the calculated dose. Data obtained from concurrent imaging would allow adjusting the variables of the model to

improve control of the process.

So far, this analysis has been successful in interpreting the lesion shapes, and demonstrating which beam patterns produce a dose distribution more favorable to lesioning the intended region.

Appendix

The focal spot size, absent any tissue aberrations, is defined by diffraction, so its area **a** is related to the transducer area **A** by

$$\mathbf{a} \cong \frac{\lambda^2 f^2}{\mathbf{A}} \qquad \text{(A1)}$$

where λ is the wavelength in the medium and f the focal distance. The *intensity gain* in a lossless medium for longitudinal waves of frequency $F = c / \lambda$ is, save a constant factor dependent on the transducer geometry,

$$\text{Gain (lossless)} = \frac{\mathbf{A}}{\mathbf{a}} \cong \left(\frac{\mathbf{A}\,F}{c\,f}\right)^2 \qquad \text{(A2)}$$

On the other hand, attenuation in a lossy medium of attenuation coefficient α dB/MHz-cm, after traversing a distance x (usually less than the focal distance) is

$$\text{Attenuation (loss)} = 10^{-(x\,\alpha\,F/10)} \qquad \text{(A3)}$$

So the net acoustic gain is the product of (A2) and (A3):

$$G = \left(\frac{\mathbf{A}\,F}{c\,f}\right)^2 10^{-(x\,\alpha\,F/10)} \qquad \text{(A4)}$$

Optimizing G is simple: it has a maximum at

$$F_0 = \frac{20}{\ln 10}\,\frac{1}{x\,\alpha} \qquad \text{(A5)}$$

and the value of G at F_0 is

$$G = 10.2\left(\frac{\mathbf{A}}{x\,\alpha\,c\,f}\right)^2 \qquad \text{(A6)}$$

•••••

References

1 **Fry, W.J., Mosberg, W.H. and Fry, F.J.** Production of Focal Destructive Lesions in the Central Nervous System with Ultrasound. *J. Neurosurg.* **11** (1954) 471-478.

2 **Fry, W.J., Barnard, J.W., Fry, F.J., Krummins, R.F. and Brennan, J.F.** Ultrasonic Lesions in the Mammalian Central Nervous System. *Science* **122** (1955) 517-518.

3 **Fry, W.J.** Intense Ultrasound in Investigations of the Central Nervous System. *In Lawrence, J.H. and Tobias, C.A. (eds.) Advances in Biological and Medical Physics.* Academic Press, New York, 1958. Vol. VI, 281-348.

4 **Sanghvi, N.T., Foster, R.S., Fry, F.J., Birhle, R., Hennige, C. and Hennige, L.V.** Ultrasound Intracavity System for Imaging, Therapy Planning and Treatment of Focal Disease. *Proc. IEEE Ultras., Ferroel. and Cont. Syst. Int. Symp.*, Arizona 1992.

5 **Hanafy, A. and Zanelli, C.I.** Quantitative Real-Time Pulsed Schlieren Imaging of Ultrasonic Waves. *Proc. 1991 IEEE Ultras. Symp.* 1223-1227.

6 **Holm, A., Persson, H.W. and Lindstrom, K.** Optical Diffraction Tomography of Ultrasonic Fields with Algebraic Reconstruction Techniques. *Proc. 1990 IEEE Ultras. Symp.* 685-688.

7 **Reibold, R. and Molkenstruck, W.** Light Diffraction Tomography Applied in the Investigation of Ultrasonic Fields. *Acustica* **56** (1984) 180-192.

8 **Arditi, M., Foster, F.S. and Hunt, J.W.** Transient Fields of Concave Annular Arrays. *Ultrasonic Imaging* **3** (1981), 37-61.